Proceedings of ICFDP9:
Ninth International Congress of Fluid Dynamics & Propulsion
December 18-21, 2008, Alexandria, Egypt

ICFDP9-EG-271

PREDICTION FOR THE MASS TRANSFER AND OXYGEN CORROSION IN COMPLEX PIPELINES

Mohamed. A. Doheim
Professor
Department of Mining and Metallurgy,
Faculty of Engineering,
Assiut University, Egypt

Hesham M. El-Batsh
Associate Professor
Mechanical Engineering Department
High Institute of Technology,
Benha University, Egypt

Ahmed F. Hassan
Inspection Sector,
Assiut Oil Refining Company (ASORC),
Assiut, Egypt

ABSTRACT

Corrosion of pipelines is a common problem in industrial organizations. The pipelines always contain elbow fittings. Generally, corrosion rate in elbows is higher than corrosion rate in straight pipes. Corrosion is governed by the flow structure and the associated mass transfer from the flow to the elbow wall. In this study, the mass transfer of oxygen is solved using numerical technique. The mass transfer coefficient in elbow relative to the mass transfer coefficient of straight pipe is calculated and compared to published experimental data and numerical predictions. The comparison showed that the preset numerical technique could accurately predict the distribution of the mass transfer coefficient in elbows. Corrosion rates are calculated for the case study of a complex pipeline configuration which exists is Assiut Oil Refining Company (ASORC), Egypt. The maximum corrosion rates in different elbows throughout the pipeline are predicted. It is found that the maximum corrosion occurs mainly at two locations. These locations exist at the outlet of the elbow namely at the elbow outer surface and at the elbow inner surface. This result agree with field observations.

KEYWORDS:

Corrosion, two phase flow, mass transfer, pipelines, numerical calculations.

INTRODUCTION

Corrosion of metallic structures has a significant impact on the economy. A report on the cost of corrosion was prepared by Battelle Columbus Laboratories and the National Bureau of Standards [1]. In this report, the cost of corrosion was estimated at more than 4 % of the gross national product.

Corrosion of the petroleum refinery pipeline networks is an important subject. Such pipeline networks usually have good design, materials and operating practices. However, pipelines do occasionally fail. The most common causes of damage and failures are due to erosion-corrosion problems [2].

The simultaneous flow of hydrocarbon and water is a common occurrence in refinery systems. The flow of hydrocarbon-water mixtures through pipelines is highly complex due to the differences in the viscosity and in the density between the water and the hydrocarbon. Groysman and Erdman [3] studied the corrosion from light petroleum distillates with different water contents. They found that petroleum distillates are not corrosive unless water and dissolved species are contained in them. The study showed that the main cause of corrosion in the petroleum distillates pipeline networks is the presence of water and the dissolved oxygen.

Corrosion is governed by the transfer of chemical species from the flowing hydrocarbon-water mixture to the pipeline walls.

The pipelines always contain fittings such as elbows, reducers and T-junctions. Generally, the rate of corrosion in fittings is higher than the rates in straight pipes.

Corrosion modeling is used to predict the rate and the location of corrosion. Clear understanding of mass transfer of chemical species is extremely important for predicting corrosion rate in hydrocarbon-water pipelines. Wang et al. [4] and Wang and Shirazi [5] calculated the mass transfer coefficient in elbows and developed correlations to predict the maximum elbow mass transfer coefficient as a function of flow parameters and elbow geometry. Kashid et al. [6] used a finite element based computational fluid dynamics (CFD) model to study mass transfer in the liquid-liquid flow. Wang and Postlethwaite [7] calculated the mass transfer and the corrosion rate by oxygen from a single-phase flow. Keating and Nesic [8, 9] presented a model to predict corrosion in a U-bend. The flow field was obtained by solving Navier Stokes equations with a turbulence model. Mass-transfer and oxygen corrosion was calculated using species concentration fields. Nesic et al. [10] presented an integrated CO_2 and H_2S corrosion model. Ferng et al. [11,12] proposed a model for the investigation of corrosion and the results showed qualitative representations for the corrosion. Bozzini et al. [13] presented numerical simulation of corrosion in a homogeneous mixture. The assumption of homogenous mixture is not precise because the difference in density and viscosity between different phases changes the flow structure and influences corrosion rate.

Previously studies in mass transfer and corrosion are performed for either a single pipe or a single elbow. In practical applications, pipelines contain several pipes and elbows and normally the distance between elbows is not sufficient to obtain fully developed flow. Therefore, each elbow in the pipeline is affected by the upstream elbows and the pipeline configuration. Accurate prediction for the corrosion in pipelines needs precise calculation for the flow field. The single-phase and the two-phase flow through complex pipeline configurations were previously studied by Doheim et al. [14, 15]. In these studies, the single phase flow through elbows was numerically calculated using different turbulence models and compared to published experimental data. The appropriate turbulence model was selected which can predict the complex flow features generated through bends. The two-phase flow was also calculated and verified using experimental data. The present study is concerned with the mass transfer of chemical species to the pipe wall and the associated corrosion. The aim of this paper is to predict the rate of mass transfer of chemical species to the surface. The mass transfer of chemical species is verified by using experimental data from the open literature. Corrosion by oxygen is simulated here and the model is applied to a case study with complex pipeline configuration which exists at ASORC. This case study aims to investigate the effect of pipeline geometry on corrosion rates.

THE MATHEMATICAL MODEL

In order to calculate mass transfer and corrosion rate, the governing equation for the fluid flow are solved. Since the flow considered in pipelines of practical applications is almost turbulent, a suitable turbulence model is needed. Then, the associated mass transfer of chemical species from the flow to the pipe wall is considered. Finally the equations governing the rate of corrosion at the surface are calculated.

The flow model is described by the transport equations which are developed from the conservation laws. Fluid flow characteristics are described by the continuity equation and momentum equations (Navier-Stokes equations). Using Reynolds averaging procedure, the governing equations for the incompressible turbulent flow are:

$$\frac{\partial u_i}{\partial x_i} = 0 \qquad (1)$$

$$\rho \frac{\partial}{\partial x_j}(u_i u_j) = -\frac{\partial P}{\partial x_i} + \frac{\partial}{\partial x_j}\left(\mu \left[\frac{\partial u_i}{\partial x_j} + \frac{\partial u_j}{\partial x_i} \right] - \rho \overline{u_i' u_j'} \right) \qquad (2)$$

where μ is the fluid viscosity, ρ is the fluid density and P is the pressure. The velocities u_i are time-averaged and consists of mean values $\overline{u_i}$ and fluctuating values u_i', and $-\rho \overline{u_i' u_j'}$ are the Reynolds stresses which are calculated using turbulence models.

In the eddy-viscosity turbulence models, the Reynolds stresses are proportional to the mean velocity gradient and the constant of proportionality is called eddy or turbulent viscosity μ_t. The shear stress transport SST k-ω model as devolved by Menter [16] falls in this category and is used in this study. The previous calculations for Doheim et al. [14] showed that this model can predict accurately the complex flow through pipeline configurations.

Mass Transfer

When a mixture of gases or liquids is contained with a concentration gradient, there will be a mass transfer as the result of diffusion from regions of high concentration to regions of low concentration. In turbulent flow systems, the diffusion rate accelerates as a result of the eddy mixing process. This effect is similar to the effect of the mixing processes which increases heat transfer and viscous action in turbulent flow. The mass transfer coefficient is defined in a manner similar to that used for defining the heat transfer coefficient, thus

$$J = \mathrm{k_m}(C_1 - C_2) \qquad (3)$$

where J is the mass flux, k_m is the mass transfer coefficient and C_1, C_2 are the concentrations through which diffusion occurs.

The Schmidt number Sc represents analogy between the velocity field and concentration field and is defined as:

$$\mathrm{Sc} = \frac{\mu}{\rho D_f} \tag{4}$$

where D_f is the mass diffusion coefficient.

In convection mass transfer problems, the Sherwood number is defined as:

$$\mathrm{Sh} = \frac{k_m D}{D_f} \tag{5}$$

where D is the diameter of the pipe.

The similarities between the governing equations for heat, mass and momentum transfer suggests that the empirical correlations for mass transfer coefficient are given in the following form:

$$\mathrm{Sh} = f(\mathrm{Re}, \mathrm{Sc}) \tag{6}$$

where Re is Reynolds number.

For pipe flow, different correlations exist for the mass transfer coefficient. Wang et al. [4] reviewed mass transfer correlations in fully developed pipe flow and they obtained from the literature the following correlation:

$$\mathrm{Sh} = 0.0165\,\mathrm{Re}^{0.86}\,\mathrm{Sc}^{0.33} \tag{7}$$

Wang et al. investigated the mass transfer coefficients in elbows and represented the results in dimensionless form using the mass transfer coefficient for straight pipes. They used the ratio of the maximum mass transfer coefficient in elbow to the mass transfer coefficient of a fully developed turbulent flow in a straight pipe (MTCRE).

$$\mathrm{MTCRE} = 0.68 + \left(1.2 - 0.044\log(\mathrm{Re})\right)e^{-0.065 r/D} + \frac{0.58}{\log(Sc + 2.5)} \tag{8}$$

where r is the radius of curvature for the elbow.

Therefore, if the mass transfer coefficient is known for a pipe, this equation can be used to estimate the maximum mass transfer coefficient in an elbow of the same diameter.

Model for Mass Transfer

In O_2 corrosion, the concentrations of chemical reacting species are dilute. Therefore, their reactions with the pipe or elbow walls do not change the flow field significantly. This assumption is considered in the present study to de-couple the flow field governing equations form those of the mass transfer and corrosion equations.

The local mass concentration of species C_i is calculated by solving the convection diffusion equation. The species conservation equation takes the following general form:

$$\rho \frac{\partial}{\partial x_j}(C_i\ u_j) = \frac{\partial}{\partial x_j}(J_i) \tag{9}$$

In turbulent flows, the mass flux is given by:

$$J_i = \left(\rho D_i + \frac{\mu_t}{\mathrm{Sc}_t}\right)\nabla C_i \tag{10}$$

where Sc_t is the turbulent Schmidt number ($\frac{\mu_t}{\rho D_t}$ where μ_t is the turbulent viscosity and D_t is the turbulent diffusivity).

The solution of the species mass transfer equation gives the concentration field of the oxygen. The local mass transfer of the species is determined from the knowledge of the diffusion coefficient and the concentration at the node adjacent to the wall. Species concentration at the wall is set at zero, and the transport is assumed to be molecular diffusion. The mass transfer coefficient, K_m, is then calculated using the local transport flow and the overall concentration difference between the bulk solution and the wall. Thus, the species mass flux from the flow to the wall, J_i, can be expressed as:

$$J_i = \mathrm{k_m}\left(C_b - C_w\right) \tag{11}$$

where C_b and C_w are the bulk and wall concentrations respectively.

The distance from the wall to the first cell is inside the mass transfer boundary layer, and the mass transfer between that point and the wall is governed by diffusive effects

$$J_i = \frac{D}{\Delta y}\left(C_i - C_w\right) \tag{12}$$

where Δy is the distance from the wall to the first cell, and C_i is the concentration at that point obtained by solving the oxygen transport equation. Therefore, the mass transfer coefficient k_m is given by:

$$k_m = \frac{D_f}{\Delta y}\frac{C_i}{C_b} \tag{13}$$

Corrosion Model

Metallic corrosion may be defined as the material deterioration that occurs when metals are exposed to reactive environments. The overall corrosion electrochemical reaction is made up of both anodic and cathodic reactions. The corrosion rate is oxygen-mass transfer controlled. In the case of iron, the anodic and cathodic reactions and oxygen corrosion can be written as: (Postlethwaite, et al. [18])

Anodic reaction

$$2Fe \rightarrow 2Fe^{2+} + 4e^{-} \qquad (14)$$

Cathodic reaction

$$O_2 + 2H_2O + 4e^{-} \rightarrow 4OH^{-} \qquad (15)$$

Corrosion rate is governed by the rate of mass transfer of chemical species from the bulk of the flow to the surface.

Therefore, if the mass transfer coefficient k_m is known, the flux of corrosive species can be determined. The oxygen corrosion rate CR (in mm/year) is calculated by using the equation given by Keating and Nesic [9] as:

$$CR = \frac{2k_m C_{bO_2} M_{\mathrm{Fe}}}{\rho_{\mathrm{Fe}}} \qquad (16)$$

where M_{Fe} is the molar mass of iron and ρ_{Fe} is the density of iron.

RESULTS AND DISCUSSION

1. Mass Transfer Verification

The experimental measurements and the numerical calculations as presented by Wang et al. [4] are used to examine the mass transfer calculations performed in this study. The data were taken in an elbow with radius of curvature to pipe diameter ratio r/D=1.5 and diameter of 70 mm for a naphthalene-air system at Schmidt number Sc=2.53. The experiments were performed at two Reynolds number as 9×10^4 and 3.9×10^5.

In the present study, the three-dimensional calculations are performed for the flow and mass transfer through the elbow. The geometry includes a straight pipe followed by a ninety degrees elbow and then a straight pipe. Three-dimensional grid with total number of cells of 312000 is used in these calculations. The inlet boundary is considered at a distance of 35D upstream of the elbow. This distance is selected to fulfill the fully developed flow at the inlet to the elbow. Uniform velocity and concentration boundary conditions are considered at the inlet. The local mass transfer coefficient is calculated for the straight pipes and for the elbow and represented in dimensionless form using Sherwood number Sh. Figures 1 and 2 show the distribution of the ratio between the elbow Sherwood number Sh to the pipe Sherwood number Sh_p along elbow outer surface at the two Reynolds numbers considered in the data. Generally, the figures show good agreements between the present results and the previous numerical calculations and experimental data presented by Wang et al.

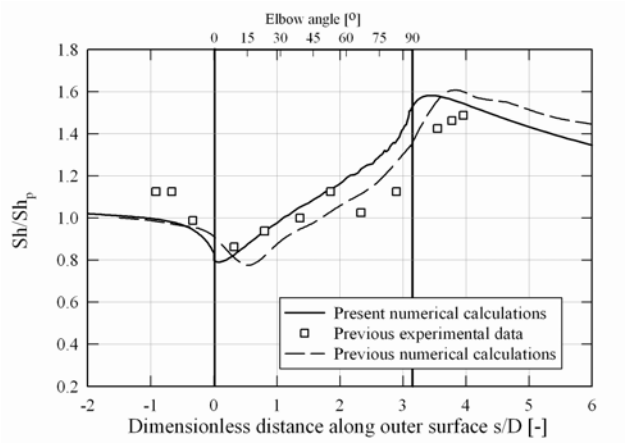

Figure 1: Present numerical calculations and previous data and calculations presented by Wang et al. [4], Re = 9 × 10^4.

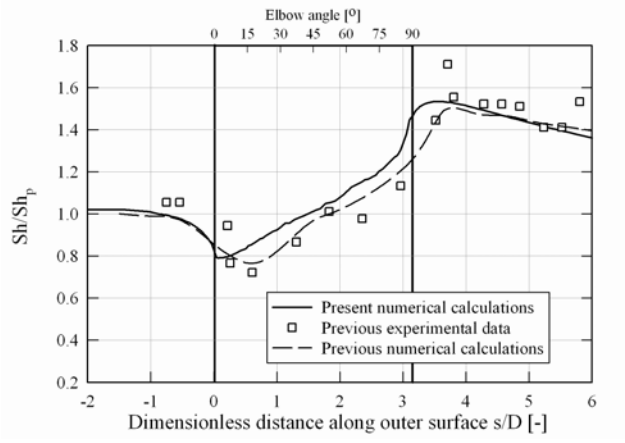

Figure 2: P resent numerical calculations and previous data and calculations presented by Wang et al.[4], Re = 3.9 × 10^5.

Figure 3 shows the static pressure coefficient C_p on the elbow outer surface which is defined as:

$$C_p = \frac{\left(P - P_{in}\right)}{0.5\rho U^2} \qquad (17)$$

where P_{in} is the inlet static pressure which is taken as the atmospheric pressure, P is the local static pressure, ρ is the fluid density and U is the fluid velocity.

The figure shows that the wall static pressure increases as the flow moves through the elbow till the angle of about 15

indicating that the flow is diffusing flow with adverse pressure gradient which is characterized by the increase in the boundary layer thickness and decrease the gradients of the velocity and the concentration of the oxygen. Figure 4 shows the velocity profile at different sections through the elbow. The figure shows that the velocity gradient at the outer surface is lower at the angle 30 in comparison to that at the inlet to the elbow. This results in the decrease in the mass transfer coefficient and Sherwood number till the angle 15 as shown in figures 1 and 2. Downstream of the angle 15, the surface pressure decreases which indicate that the flow is accelerating which has the characteristic of decreasing the thickness of boundary layer. This increases the gradients of the velocity as clear in figure 4 and the associated concentration of oxygen resulting in the increase in the mass transfer coefficient and Sherwood number as shown in figures 1 and 2.

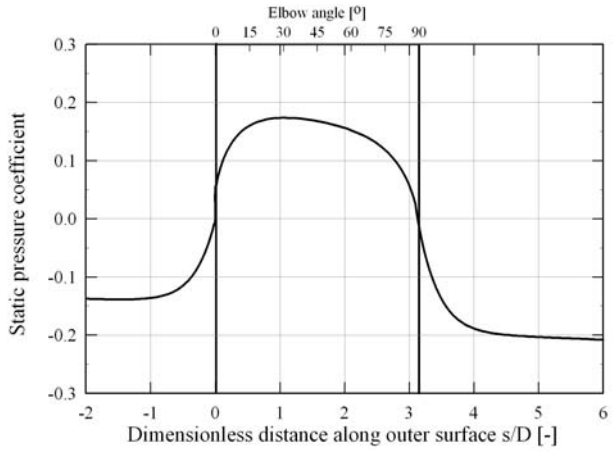

Figure 3: Pressure coefficient at the outer surface, Re = 9 × 10^4.

2. Corrosion by Oxygen in ASORC Pipeline

The selected pipeline contains lines and elbow fittings and suffers from corrosion problems during relatively short periods. The pipeline of ASORC contains six straight pipes all have the same diameter and includes five-ninety degrees elbows. Complete description about the pipeline can be found in Doheim et al. [14].

The numerical calculations are performed using computational grid with about 490000 cells. Figure 5 shows the geometry of the pipeline and the grid at a selected elbow. The grid dependency is checked and with this number of cells, it is found that the solution is grid-independent.

During normal operation, the pipeline carries a mixture of naphtha and water. The primary liquid is naphtha with about 90 % mass fraction. The inlet flow velocity is obtained from the mass flow rate through the pipeline and the density of naphtha and pipe cross-section area. Uniform velocity distribution is applied at the inlet. The properties of the naphtha are measured in the field and are used here in the calculations. The calculations are performed for different operating conditions namely the design, full and two part load conditions. In addition, different water mass fractions are used to investigate its effect on the corrosion rate. These calculations are performed at the full capacity of the pipeline. Tables 1 and 2 show operating conditions and water contents considered in this study.

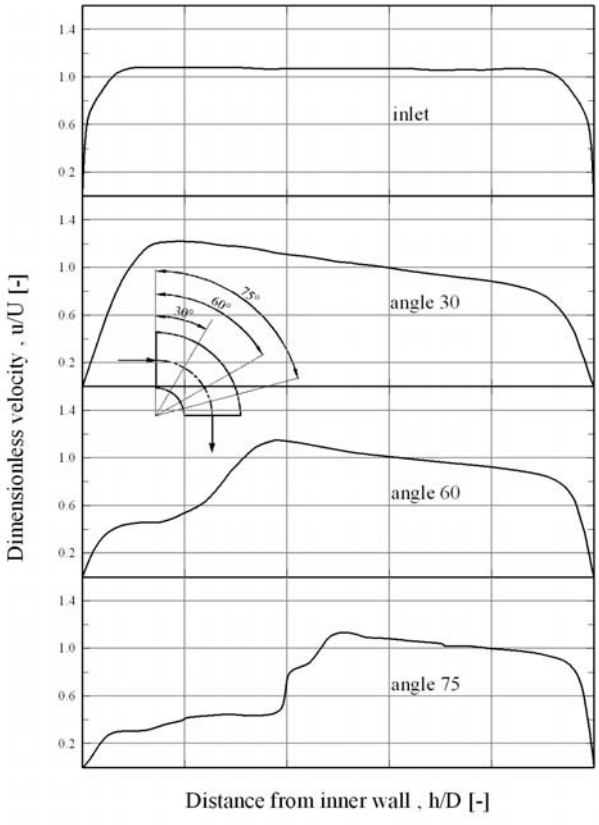

Figure 4: Velocity profile through the elbow.

Table 1: Operating conditions of ASORC

	Velocity [m/s]	Reynolds number
Design	0.21	9.3×10^4
Full	0.19	8.4×10^4
90 % part load	0.17	7.5×10^4
80 % part load	0.15	6.7×10^4

Table 2: Different water contents of ASORC

Water contents	Velocity [m/s]	Reynolds number
5 %	0.19	8.7×10^4
10 %	0.19	8.4×10^4
15 %	0.19	8.2×10^4

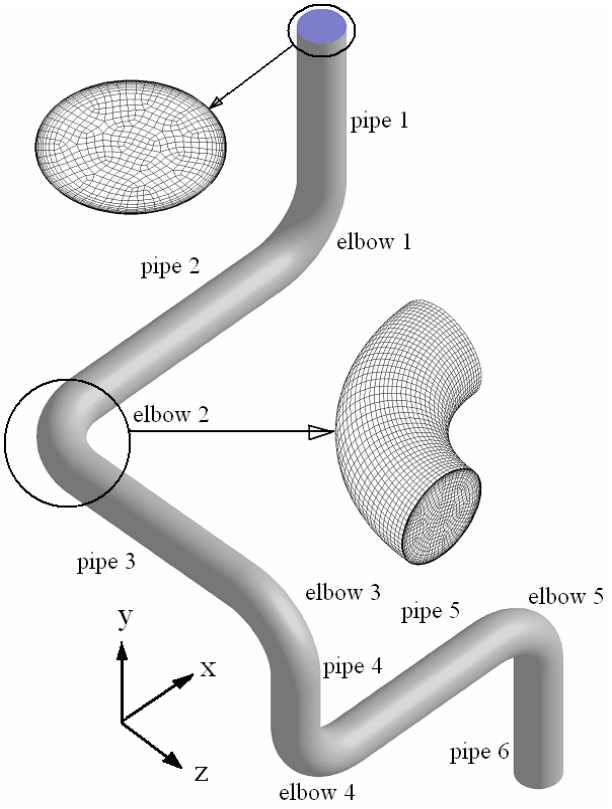

Figure 5: Computational grid of the pipelines of ASORC.

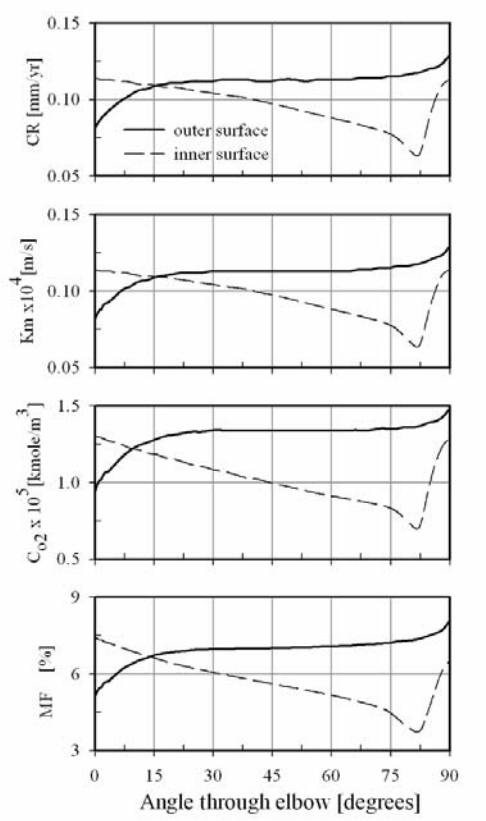

Figure 6: Parameters affecting corrosion rate at elbow 1.

The results presented here represent the corrosion rates calculated at different elbows. The flow features affecting the corrosion are extensively explained for elbow 1 while the main features of the pipeline configuration affecting corrosion rates in the remainder elbows are briefly explained. Generally, the density of the water is greater than that for the naphtha and therefore, the water is collected at the outer surface of the elbows.

Figure 6 shows the parameters which affect corrosion rate in elbow 1 of ASORC pipeline at the full capacity. At this case study, the water mass fraction is 10 % and velocity of the water-naphtha mixture is 0.19 m/s. The concentration of oxygen is 8 ppm. The data are drawn on the inner and on the outer surface through the elbow. The figure shows that the water mass fraction MF increases at the outer surface with the angle through the elbow. This result is attributed to the centrifugal force which moves the water towards the outer surface of the pipe due to its high density. The centrifugal force also decreases the water mass fraction at the inner surface of the elbow as shown in figure. The increase in the water mass fraction at the inner surface near the outlet of the elbow is caused by the secondary flow generated in the elbow. The effect of the secondary flow on the two-phase flow is extensively explained in Doheim et al. [15].

The concentration of the oxygen C_{O2} has the same trend of the water content. The oxygen is transported through the water because it is not dissolved in naphtha. This observation agrees with Groysman and Erdman [3]. They found in their study that the pure petroleum distillates are not corrosive and the water is the main reason for the corrosion of pipelines. The flow in the outer side is accelerating with the feature of decreasing the boundary layer thickness as explained above and the associated effect is an increase in the mass transfer coefficient k_m. Consequently, the corrosion rate CR increases at the outer surface with the angle of the elbow reaching the maximum at the exit.

The mass transfer coefficient in the inner surface is affected by two counter effects. The first one is the increase in the boundary layer thickness which decreases the concentration gradient and results in the decrease in the mass transfer to the surface. The other effect is the increase in the mass transfer caused by the secondary flow generated by the flow deflection through the elbow. The resultant mass transfer coefficient depends upon the contribution of each affect. In the first half of the elbow, the increase in the boundary layer thickness has the dominant effect which causes the decrease in the mass transfer coefficient. After the angle of about 80 degrees from the inlet,

the secondary flow has the dominant effect and therefore, increases the mass transfer coefficient. Corrosion rate depends upon the mass transfer of oxygen. Consequently, the distribution of the corrosion rate has the same trend of the mass transfer coefficient.

Table 3 shows the ratio of the maximum mass transfer coefficient in ASORC elbows to the mass transfer coefficient in a fully developed pipe flow (MECRE) calculated using the correlation obtained from Wang et al. [4] (equation 8) and the present numerical results. The table shows very good agreements between the numerical calculations and the correlation prediction for elbow 1. The smallest error is obtained in elbow 1 because it receives fully developed flow from the upstream pipe while the elbows from 2-5 receives the flow which is affected by the upstream elbows and results in deviation from correlation prediction.

Table 3: Comparison between numerical calculations and correlation prediction

Reynolds number	8.4×10^4	
MTCRE	Value [-]	Error [%]
Elbow 1	1.683	7.5
Elbow 2	1.632	10.3
Elbow 3	1.662	8.7
Elbow 4	1.650	9.3
Elbow 5	1.643	9.7
Correlation prediction	1.82	--

Three water mass fractions are considered in this study: the mass fraction during normal operation which is 10 %; and two different values as increasing the water mass fraction to 15 % and decreasing the water mass fraction as 5 %.

Figure 7 shows the effect of water content on corrosion rate CR of ASORC pipeline. The figure shows corrosion in the inner and in the outer surface of the elbows. Generally, increasing the water mass fraction MF increases the corrosion rate for all elbows at the inner and at the outer surfaces. This is attributed to the increase in the mass transfer from the water to the surface. The maximum CR occurred at the outer surface of the elbow and at the exit.

For any water content, corrosion rates increase in the outer surface with the flow direction till the angle of 15 degree. Then they reach constant values until the angle of almost 80. The corrosion rates then increases. For the inner surface, the corrosion rates decrease with the flow direction from the inlet to the angle of 80 degrees and then they increase dramatically.

For the same water content, corrosion rates at the outer surfaces show the same trend and the same level for all elbows. For the inner surfaces of the elbows, the corrosion rates show different trends and levels near the outlet which is caused by the secondary flow generated through the elbows. The maximum CR at the inner surface is obtained in elbow 1 which receives fully developed flow from the upstream pipe. For the downstream elbows from 2 to 5, the secondary flow generated in each elbow when added to the upstream secondary flow generated in the upstream elbow(s) reduces CR.

Figure 8 shows corrosion rates at different elbows of the pipeline at various loading. Different inlet velocities are considered namely 0.15, 0.17, 0.19 and 0.21 m/s. The figure shows that increasing the pipeline loading increases corrosion rates in all elbows. This result is attributed to the increase in the mass transfer of oxygen species from the water to the pipeline wall. The increase in mass transfer coefficient of oxygen is supported by the correlations given by Wang et al. [4]. Increasing the flow velocity through the pipeline increases Reynolds number and increases the Sherwood number and the mass transfer coefficient.

CONCLUSIONS

The turbulent flow field was calculated in this study through complex pipelines by solving Reynolds Averaged Navier-Stokes Equations. A mass transfer model was used to calculate the transfer of oxygen species from the flow to the pipe wall. The mass transfer coefficient calculated from the present study was compared to the previous experimental and numerical calculations for the flow through a ninety degrees elbow. It was found that the maximum mass transfer coefficient occurs at the elbow outer surface near the outlet.

The flow was solved for more complicated pipeline geometry with five elbows and six straight pipes. The flow was solved for the napthta-water mixture. The model was also extended to calculate corrosion rates. The results showed that the maximum corrosion in elbows occurs at the outer surface of the elbows near the exit. The effect of water content and the pipeline loading were examined. It was concluded that increasing the water content in the pipeline increases corrosion rates. It was concluded also that increasing the loading through the pipeline increases corrosion rates which was attributed to the increase in Reynolds number and Sherwood number and the associated mass transfer coefficient.

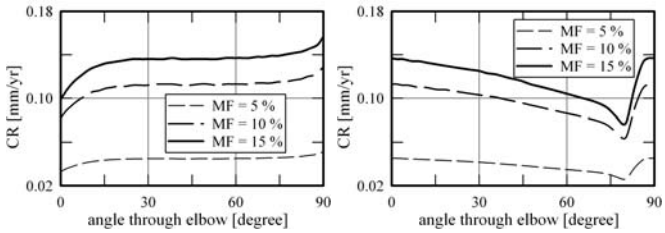

elbow 1

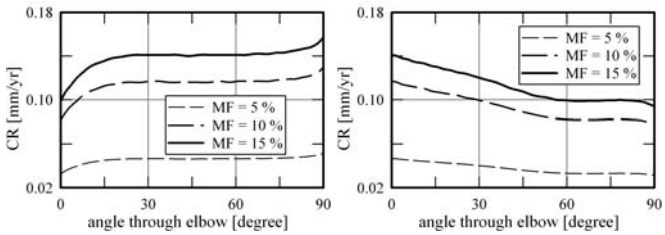

elbow 2

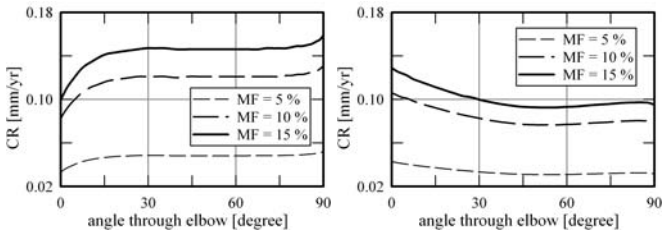

elbow 3

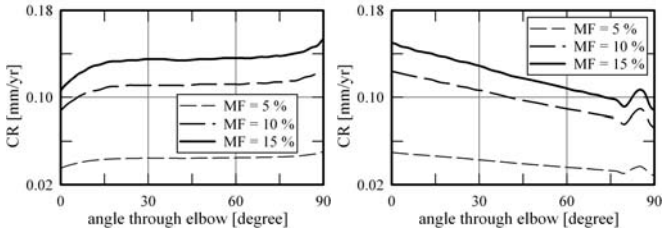

elbow 4

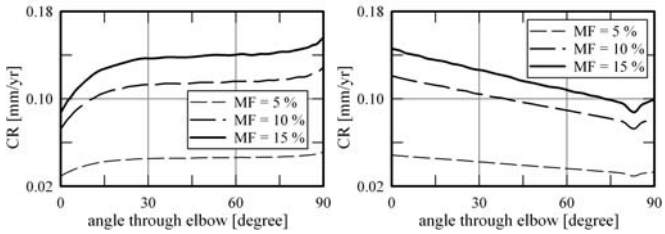

elbow 5

Outer surface **Inner surface**

Figure 7: Effect of water content on elbows corrosion rates.

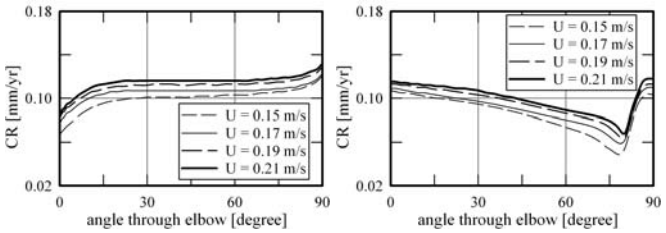

elbow 1

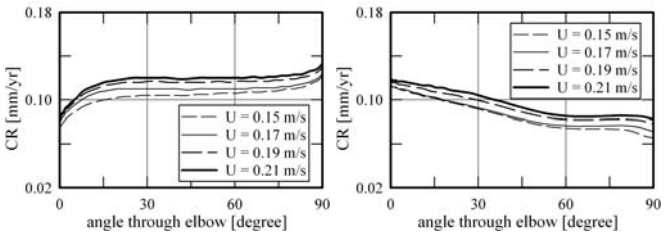

elbow 2

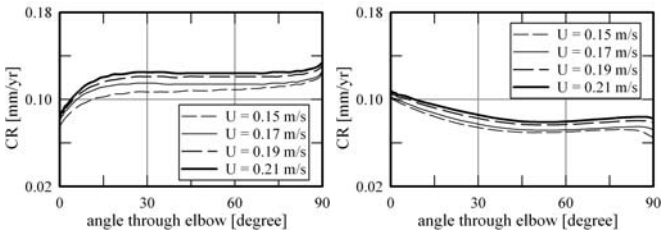

elbow 3

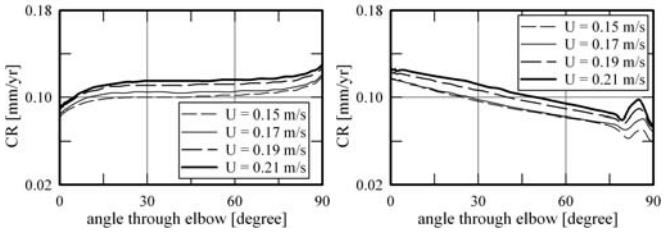

elbow 4

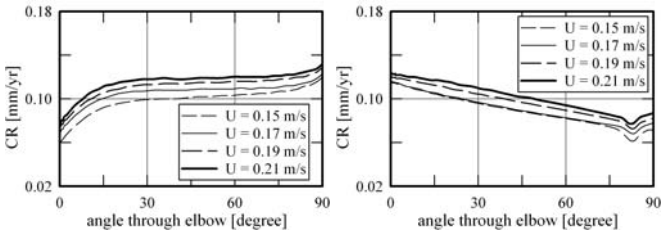

elbow 5

Outer surface **Inner surface**

Figure 8: Effect of pipeline loading on elbows corrosion rates.

NOMENCLATURE

C	Concentration
C_i	Local concentration
C_b	Bulk concentration
C_p	Static pressure coefficient
C_w	Wall concentration
CR	Corrosion rate
D	Pipe diameter
D_f	Mass diffusion coefficient
D_t	Turbulent diffusivity
J	Mass flux
k_m	Mass transfer coefficient
M_{Fe}	Molar mass of iron
P_{in}	Inlet static pressure
P	Static pressure
r	Radius of curvature
Sh	Sherwood number
Re	Reynolds number
Sc	Schmidt number
Sc_t	Turbulent Schmidt number
u_i	Time-averaged velocity
$\overline{u_i}$	Mean velocity
u_i'	Fluctuating values
U	Fluid bulk velocity
Δy	Distance from the wall to the first cell
μ	Fluid viscosity
μ_t	Turbulent viscosity
$-\rho\overline{u_i'u_j'}$	Reynolds stresses
ρ	Fluid density
ρ_{Fe}	Iron density

ACKNOWLEDGMENTS

The authors acknowledge the support of ASORC in providing technical assistance and submitting required data throughout this study.

REFERENCES

[1] http://www.corrosioncost.com/

[2] Cosham, A., Hopkins, P., Macdonald, K., Best practice for the assessment of defects in pipelines – Corrosion, Engineering Failure Analysis, 12 (7), 2007, pp.1245-1265.

[3] Groysman, A. and Erdman, N., A study of corrosion of mild steel in mixtures of petroleum distillates and electrolytes, Corrosion vol. 56, no. 12, December 2000, pp. 1266-1271.

[4] Wang, J., Shirazi, S.A., Shadley, J.R., Rybicki, E.F. and Dayalam, E., A correlation for mass transfer coefficients in elbows, Corrosion 1998, Proceedings of the NACE, paper no. 42.

[5] Wang, J. and Shirazi, S.A., A CFD based correlation for mass transfer coefficient in elbows, International Journal of Heat and Mass Transfer, vol. 44, 2001, pp. 1817-1822.

[6] Kashid, M. N.; Agar, D. W. and Turek, S., CFD modeling of mass transfer with and without chemical reaction in the liquid-liquid slug flow capillary microreactor, Accepted for publication in the Chemical Engineering Science.

[7] Wang, Y. and Postlethwaite, J., The application of low Reynolds number k-ε turbulence model to corrosion modeling in the mass transfer entrance region, Corrosion Science, vol. 39, no. 1, 1997, pp. 1265-1283.

[8] Keating, A. and Nesic, S., Prediction of two-phase erosion-corrosion in bends, Second International Conference on CFD in the Minerals and Process Industries, CSIRO, Melbourne, Australia, 6-8 December 1999.

[9] Keating, A. and Nesic, S., Numerical prediction of erosion-corrosion in bends, Corrosion, vol. 57, no. 7, 2001, pp. 621-633.

[10] Nesic, S., Cai, J. and Lee, K.L.J., A multiphase flow and internal corrosion prediction model for mild steel pipelines, Corrosion 2005, paper No. 05556.

[11] Ferng, Y.M., Ma, Y.P. , Ma, K.T. and Chung N.M. , A new approach for investigation of erosion-corrosion using local flow models, Corrosion, April 1999, pp. 332-342.

[12] Ferng, Y.M., Ma, Y.P. and Chung, N.M., Application of local flow models in predicting distributions of erosion-corrosion locations, Corrosion, February 2000, pp.116-126.

[13] Bozzini, B., Ricotti, M.E., Boniardi, M., Mele, C., Evaluation of erosion–corrosion in multiphase flow via CFD and experimental analysis, Wear 255, 2003, pp. 237–245.

[14] Doheim, M.A., El-Batsh, H. M., Hassan, A.F., Hydrodynamic investigation of single-phase flow in complex pipeline configurations with reference erosion-corrosion, The 10th International Mining, Petroleum, and Metallurgical Engineering Conference, March 6-8, 2007.

[15] Doheim, M.A., El-Batsh, H. M., Hassan, A.F., Hydrodynamic investigation of two-phase flow in complex pipeline configurations with reference erosion-corrosion, The 10th International Mining, Petroleum, and Metallurgical Engineering Conference, March 6-8, 2007.

[16] Menter, F., Two-equation eddy-viscosity turbulence models for engineering applications, AIAA Journal, vol. 32(8), pp. 1598-1605, 1994.

[17] Manninen, M., Taivassalo, V. and Kallio, S., On the mixture model for multiphase flow, VTT Publications 288, Technical Research Centre of Finland, 1996

[18] Postlethwaite, J. Dobbin, M.H. and Bergevin. K., The role of oxygen mass transfer in the erosion-corrosion of slurry pipelines, corrosion, 42(9), pp. 514-521, 1986.